applied sciences

MDPI

Article

Mechanical Behavior of Large-Diameter Adjacent Shield Tunnelling Bridge Piles: A Case Study of Chunfeng Tunnel

Jingang Wu [1,2], Jinpeng Zhao [1,*], Zhongsheng Tan [1], Xiangyu Liu [2], Xia Wang [2] and Minggao Liu [2]

[1] Key Laboratory of Urban Underground Engineering of Ministry of Education, Beijing Jiaotong University, Beijing 100044, China; 21114115@bjtu.edu.cn (J.W.); zhshtan@bjtu.edu.cn (Z.T.)
[2] Beijing General Municipal Engineering Design and Research Insititute Co., Ltd., Beijing 100082, China; m13810430866@163.com (X.L.); m18813058046@163.com (X.W.); z13383417454@163.com (M.L.)
* Correspondence: 18115060@bjtu.edu.cn

Abstract: When a large-diameter shield crosses through bridge piles, stress and deformation of the bridge piles caused by tunnel excavation occurs. This is a an exciting topic of engineering research into the construction of subways. We considered an 15.8 m large-diameter shield machine made in China to excavate the Chunfeng tunnel as the background of our research. First, based on the previous engineering experience, reinforcement measures of the shield crossing the bridge piles were investigated. PLAXIS 3D finite element software was used to simulate the process of shield tunnelling through the piles of Hongling Interchange No. 1 Bridge. We analyzed the mechanical characteristics of the piles in the process of shield tunnelling through the bridge piles and evaluated the reliability of the reinforcement measures. Finally, combined with field monitoring data, the accuracy of the model and the rationality of the treatment measures were verified. This research considered a successful case of 15.8 m large-diameter adjacent shield tunnelling bridge piles. Analysis of the stratum and the mechanical behavior of bridge piles in the process of crossing provides a theoretical reference for engineering measures on similar projects in the future.

Keywords: large diameter shield; crossing bridge piles; mechanical behavior; numerical simulation; field monitoring

Citation: Wu, J.; Zhao, J.; Tan, Z.; Liu, X.; Wang, X.; Liu, M. Mechanical Behavior of Large-Diameter Adjacent Shield Tunnelling Bridge Piles: A Case Study of Chunfeng Tunnel. *Appl. Sci.* **2022**, *12*, 5418. https://doi.org/10.3390/app12115418

Academic Editor: Daniel Dias

Received: 22 April 2022
Accepted: 25 May 2022
Published: 27 May 2022

1. Introduction

The shield tunnel construction method has been well applied and developed in urban rail and the construction and development of urban rail transit because of its high safety, high degree of mechanization, and little impact on ground traffic [1,2]. However, excavation of a shield tunnel causes stratum loss. If the tunnel is close to existing buildings and structures such as bridge piles, it can lead to the deformation of existing bridge piles and harm the safety of existing bridges [3–5]. Due to the large excavation area, extensive construction disturbance range, and strength of the large-diameter shield, the work has a significant and adverse impact on existing bridge piles [6]. Therefore, research on the stress and deformation of deep foundations (e.g., piles) caused by tunnel excavation is a relevant and exciting topic in subway construction.

At present, research on shield crossing bridge piles mainly adopts the methods of theoretical analysis [7,8], model testing [9], numerical simulation [10,11], and field monitoring [12,13]. Huang et al. [7] studied tunnel side piles related to fluid-structure coupling. The results showed that the groundwater on both sides of the surface presents a "U" flow trend to the upper part of the tunnel, vertical displacement of the pile results in settlement of the upper pile and upward deformation of the lower pile, and horizontal displacement of the pile presents a continuous "S" distribution. Wang et al. [12] showed that the expansion and reinforcement of the raft foundation of Fengqi Bridge and the improvement of the composite ground effectively reduced bridge settlement during tunnelling and improved

the mechanical conditions of the bridge structure. He et al. [14] studied the response of different minimum distances between pile groups and tunnel centerlines in clay using physical scale model tests and three-dimensional nonlinear finite element models. Wang et al. [15] established a three-dimensional finite element model of pile foundation construction of a large-diameter shield side crossing viaduct using the finite element method, developed an additional response of viaduct pier and pile during construction, and demonstrated the protection measures of viaduct pile foundation involved in the project. The above research mainly focused on the problem of conventional diameter shield crossing through buildings and structures. There is little research on large-diameter (especially 16 m-level) slurry shield tunnel construction on the surrounding soil and structure.

Due to the large diameter of the slurry shield studied in this paper, the tunnel disturbance to the surrounding soil and structure was the main problem during design and construction, especially with respect to the two bridge piles of Hongling Interchange No. 1 Bridge. Prior experience with this type of slurry shield tunnelling project is relatively limited. Our research considered a 15.8 m large-diameter shield machine made in China to excavate the Chunfeng tunnel as the background of the study. First, based on previous engineering experience, reinforcement measures of shield crossing of bridge piles was considered. Based on this, PLAXIS 3D finite element software was used to simulate the process of shield tunnelling through the piles of Hongling Interchange No. 1 Bridge, analyze the mechanical characteristics of the piles in the process of shield tunnelling through the bridge piles, and evaluate the reliability of the reinforcement measures. Finally, combined with field monitoring data, the accuracy of the model and the rationality of the treatment measures were verified.

2. Engineering Background

2.1. Project Overview

The Chunfeng tunnel project is a significant transportation project of Shenzhen's Eastward Strategy. It is designed according to the technical standards of an urban expressway [16], with a total length of about 5.1 km. The plan of the line is shown in Figure 1. The total length of the underground road (tunnel) is about 4.3 km, and the length of the shield section is 3.58 km. The tunnel adopts a double-layer structure of a single tunnel, and the upper and lower layers can accommodate two-way traffic (see Figure 2). A super large-diameter slurry balance shield with a diameter of 15.8 m was used for tunnelling in the shield section. In April 2019, as China's largest slurry shield tunnel, it was also the first motor vehicle tunnel constructed by shield technology and the first single tunnel double-layer motor vehicle tunnel in Shenzhen. The shield machine of the Chunfeng tunnel started smoothly.

Figure 1. Plan of the line.

Figure 2. Cross-section of the shield tunnel.

2.2. Large-Diameter Slurry Shield

Figure 3 shows the super large diameter slurry balance shield used in the Chunfeng tunnel project. The shield was developed by the China Railway Engineering Equipment Group Co., Ltd. It is equipped with a normal pressure tool change, a main drive expansion, swing, tool wear protection and monitoring, and anti-mud cake with a scouring system [17]. The shield machine first uses a double crushing and grading slag soil treatment technology based on multi-stage treatment. A gear roller crusher is set in front of a slurry discharge pump for graded crushing of slag and stone and for increasing the particle size of slag discharge, which effectively reduces the risk of blocking and delayed discharge in the air cushion bin. Because of the construction risk of the section with a small curve radius (R = 750 m), the shield machine manufacturer developed a small curve tunnelling jamming early warning system, which successfully assisted the shield machine in completing this section. A shield was used in the Chunfeng tunnel project, with a maximum excavation of 12 m in a single day and an average excavation rate of 6 m/d. This represents the technical level of large-diameter slurry shield tunnel construction in China.

Figure 3. Slurry shield of the Chunfeng tunnel.

2.3. Engineering Geology

More than 80% of the geology of the tunnel crossing is a hard rock section underlying bedrock. The rock strata of the crossing section mainly includes granite, tuffaceous sandstone, cataclastic rock, schist and metasandstone. The maximum compressive strength of slightly weathered schist rock is 240 MPa. Medium permeable pressure bearing water exists in bedrock and structural fractures. The engineering geological profile is shown in Figure 4. The buried depth of the tunnel is 24~62 m. Considering the construction scale and difficulty, the Chunfeng road tunnel is the first of its kind in China [17].

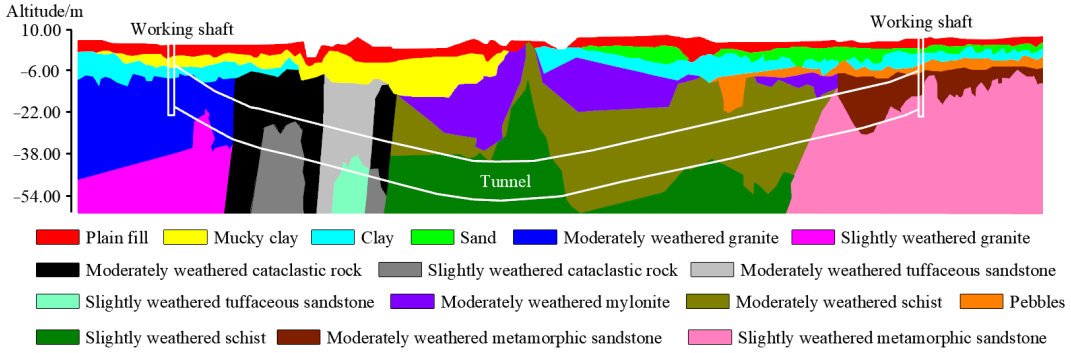

Figure 4. Engineering geological profile.

2.4. Problems and Solutions Encountered in Tunnel Excavation

The shield machine of the Chunfeng tunnel is located between pile #2 and pile #3 of No. 1 bridge of the Hongling Interchange, 40 m after its start. The plane distance between the tunnel and pile #2 and pile #3 is 2.4 m and 4.3 m, respectively. The top elevation of the shield structure is −4.92 m, and the bottom elevations of pile #2 and pile #3 are −20.2 m and −21.2 m, respectively. Relative position relationship is shown in Figure 5. Here, the stratum is mainly plain fill, muddy clay, medium sand, gravelly sand, moderately weathered granite, and slightly weathered granite. The stratum crossed by the tunnel is mainly moderately weathered granite. The bearing stratum at the pile ends of pile #2 and #3 is moderately weathered granite.

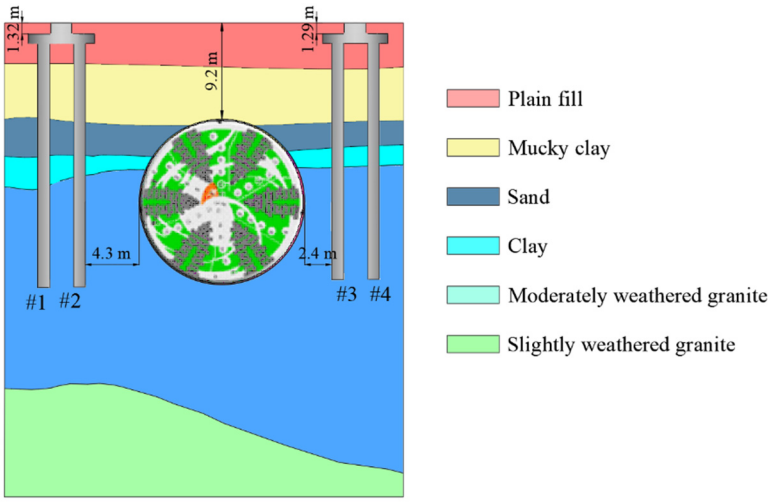

Figure 5. Relative relationship between shield tunnel and bridge piles.

Considering the problem of large-diameter adjacent shield tunnelling bridge piles, combined with the treatment experience of previous similar engineering problems [18], a scheme for strengthening the soil around the pile foundation needed to be proposed.

The shield passes through the bridge piles of Hongling Interchange No. 1 bridge within about 16 m of Chainage ZK0 + 875~ZK0 + 890. The location of the grouting hole is shown in Figure 6. Before shield tunnelling, the soil around the pile foundation were reinforced by sleeve valve pipe grouting. The grouting holes were arranged in a quincunx shape with a spacing of 1 m × 1 m. The length of the grouting pipe near the bridge pile must be driven into the moderately weathered granite layer for 1 m. The water-cement ratio of cement slurry used for grouting is 0.5:1~1:1. The initial grouting pressure is 0.5~0.4 MPa. After the grouting pressure gradually rises to 0.5~0.8 MPa, it is necessary to continue grouting for 10 min. The grouting effect verification index is that the unconfined compressive strength of grouting reinforced bodies for 28 days should be higher than 1.0 MPa, and its permeability coefficient less than 1.0×10^{-7} cm/s.

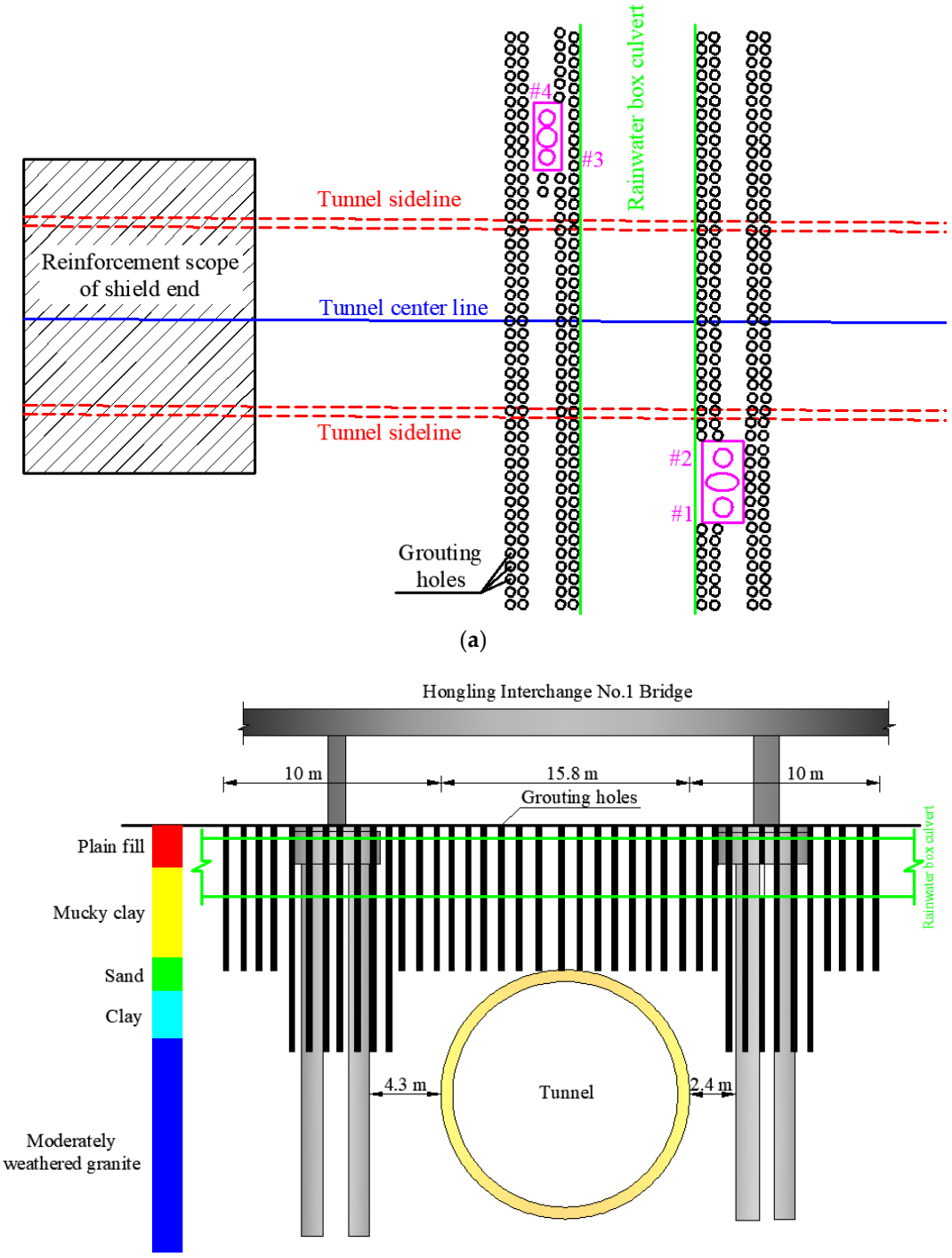

Figure 6. Grouting reinforcement scheme. (**a**) Plan of the grouting reinforcement scheme. (**b**) Section of the grouting reinforcement scheme.

3. Numerical Simulation of Mechanical Behaviour of Large-Diameter Adjacent Shield Tunnelling Bridge Piles

It is known from the current research results that in the process of adjacent shield tunnelling bridge piles, stress redistribution of soil mass is caused by disturbing the surrounding soil layer, which affects the stress, deformation and bearing characteristics of adjacent piles [19]. If the displacement of the pile body is too large, or uneven settlement is large, this would cause cracks in the overlying bridge, which would affect the durability

and regular use of the bridge [20]. In addition, the relative positions between the pile toes and the tunnel determine the disturbance of the pile. Excessive settlement usually occurs when the pile toes are above the tunnel. If the pile toes are embedded deeper than the tunnel, the main problem is related to the additional bending of the pile. When the super large diameter shield of the Chunfeng tunnel adjacent crosses the bridge piles, the impact of the bridge piles must be evaluated and predicted in advance. The deformation control standard of piles also needs to be determined to evaluate the safety of the existing bridge in shield tunnelling.

3.1. Bridge Piles Deformation Control Standard

Combined with relevant specifications of Chinese tunnels [16] and previous underpass cases [21], the control values of deformation are shown in Table 1.

Table 1. Deformation control standard.

Control Items	Range of Control Items	References
Surface settlement	+10 mm~−30 mm	Sheng et al., [21]
Pier settlement	≤15 mm	Xu et al., [22]; He et al., [14]
Pier settlement speed	±3 mm/day	
Differential settlement between longitudinal adjacent piers	≤2 mm	Mohamad et al., [23]; Liu et al., [24]; Liu et al., [25]
Differential settlement between transverse adjacent piers	≤3 mm	

3.2. Establishment of Numerical Model

The finite element software PLAXIS 3D was used for numerical calculation, with a model size of 90 m × 120 m × 40 m (see Figure 7). The tunnel lining and bearing platform were simulated by solid elements. This paper mainly focuses on the responses between the piles and the tunnel. The simplified modelling of the lining was carried out by numerical simulation, and the influences of the segmented lining on the piles were not considered [26,27]. The pile body was simulated by an Embedded Pile structural element, which is a friction end bearing pile with a length of 23 m and a diameter of 1.2 m. The interaction between the pile and soil layers was determined through the coupling layer between the pile and soil layers. The coupling layer embedded in the pile element defaults to the stiffness and friction parameters in PLAXIS 3D. In order to obtain more accurate results, the elements near the piles were densified to make the grid size no more than 1 m. The load on the pile foundation is divided into two parts, one is the dead weight of the bridge, the other is the lane load and crowd load. The dead load of the bridge acting on each pile top was considered to be 1MN, and the movable load of vehicles was considered to be 200 kN. The load calculated according to relevant specifications was added to the foundation, and the load of each part of the model was determined in PLAXIS 3D [16].

To better simulate the interaction between the tunnel, soil layers and bridge piles, all soil layers were simulated by a small-strain Hardening-Soil constitutive model. The hardened soil model was developed by Schanz [28] and then extended to the small strain range by Benz [29]. It is one of the most advanced soil constitutive models, and has been successfully used in deep foundation pits, large foundation rafts, diaphragm or sheet pile walls, and other applications, in the past decade [30,31]. The small strain Hardening-Soil model considers the volumetric and shear hardening mechanism. The deformation characteristics of the soil in the initial stage of the constitutive model are not entirely linearly elasticity but elastic-plastic deformation with high modulus is affected by stress history and loading path. Fully considering the nonlinear characteristics of the soil under small strain, the constitutive model can better reflect the interaction between soil and structure under a working load [32]. In combination with the tunnel geological survey data [33] and relevant specifications [16], the soil layer parameters are shown in Table 2. The empirical relationship between E_{50}^{ref} and E_{ur}^{ref}, refer to the Plaix 3D manual [34]. Poisson's ratio is

determined by the triaxial drained loading and unloading test. The reference pressure of the power exponent *m* of the stiffness stress level correlation is 100 kPa. It is worth noting that the effect of grouting reinforcement is achieved by increasing the soil modulus of the corresponding reinforced stratum [35].

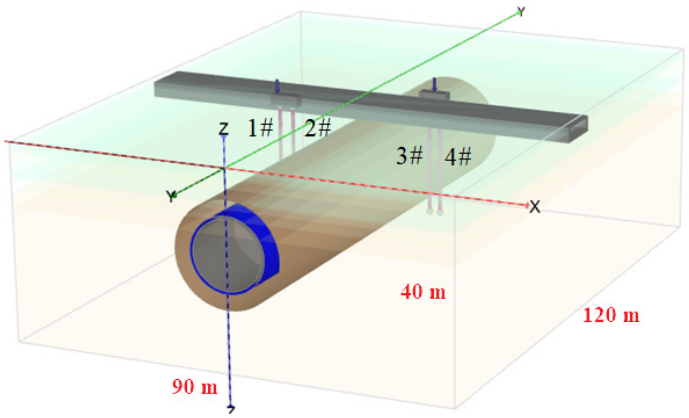

Figure 7. PLAXIS 3D finite element model.

Table 2. Physical and mechanical parameters of the soil layer.

Model Parameters		Plain Fill	Clay	Medium Sand	Gravel Sand	Moderately Weathered Granite	Slightly Weathered Granite
Secant modulus corresponding to partial stress of 0.5 times shear strength under reference stress	E_{50}^{ref} (MPa)	8	6	17	24	100	120
Unloading and reloading modulus under	E_{ur}^{ref} (MPa)	24	18	51	72	300	360
Gravity of unsaturated soil	γ_{unsat} (kN/m^3)	18.4	17.2	19	20	19.7	20.9
Gravity of saturated soil	γ_{sat} (kN/m^3)	20	20.3	20	20	23.3	24.5
Poisson's ratio	ν	0.3	0.46	0.28	0.25	0.22	0.20
Cohesion	c (kPa)	28	25	0	0	35	100
Friction angle	φ (°)	19	21	28	30	33	35
Power exponent of stiffness stress level correlation	m	0.6	0.8	0.5	0.5	0.5	0.5
Shear strain corresponding to the secant shear modulus attenuation of 0.7 times of the initial shear modulus	$\gamma_{0.7}$ (10^{-4})	2.1	2.5	2.7	1.5	1.2	1.0
Reference initial shear modulus of small strain	G_0^{ref} (MPa)	65	74	85	120	500	750
Damage ratio	R_f	0.8	0.8	0.8	0.8	0.8	0.8

The shell element in PLAXIS 3D simulates the shell material of the shield machine, and the solid element simulates the segments. The linear elastic model parameters of the shield machine shell and segments are shown in Tables 3 and 4.

Table 3. Shield machine shell parameters.

Model Parameters		Shield Shell
Modulus of elasticity	E_1 (GPa)	210
Poisson's ratio	ν_1	0.20
Gravity	γ_1 (kN/m^3)	76.5

Table 4. Tunnel segment parameters.

Model Parameters		Shield Shell
External diameter	D (m)	15.2
Internal diameter	d (m)	13.9
Thickness	t (m)	0.65
Gravity	γ_2 (kN/m^3)	27
Modulus of elasticity	E_2 (GPa)	31.0
Poisson's ratio	ν_2	0.1

The tunnel face support stress P is subject to the stable earth pressure of the heading face; its empirical formula [36] is shown in Equation (1).

$$P = K_0\gamma' H + p_w \pm 20 \quad (1)$$

where K_0 is the coefficient of static earth pressure, γ' is the effective weight of soil, H is the overburden thickness of tunnel vault, p_w is water pressure, and 20 kPa is the fluctuating pressure. The calculation shows that the support force at the vault face is 148 kPa, and the pressure gradient is determined according to the gradient setting in the actual shield tunnelling process, which is 7 kPa/m. Through relevant literature research and field data analysis [37], the grouting pressure at the shield tail was found to be 1.2 times the supporting force at the vault face. Therefore, the grouting pressure P_0 at the vault is 177.6 kPa, and the pressure gradient is 16.7 kPa/m.

The simulation process is as follows: (1) generation of initial in-situ stress field; (2) loading piles, including activated pile caps and Embedded Pile structural elements; (3) displacement of the previous stage of the model is cleared to 0, and the grouting reinforcement area is activated at the same time; (4) activation the installed lining, shield machine and segments; (5) for the first ring of shield excavation, activate the tunnelling parameters, including heading face force, jack thrust and grouting pressure; (6) in the second ring of shield excavation, freeze the tunnelling parameters of the previous stage and activation the tunnelling parameters of the new stage and segments of the previous stage; (7) by analogy, freeze the tunnelling parameters of the previous stage and activate the tunnelling parameters of the new stage.

In the numerical simulation process, the cutter head of shield machine at the first ring of excavation is 22 m away from the pile foundation to ensure that the excavation can be carried out before the shield starts to affect the pile foundation. After the shield tail is 20 m away from the pile foundation, the excavation is completed to ensure that the pile foundation has been separated from the influence range of the shield.

3.3. Analysis of Numerical Simulation Results

In order to evaluate the effect of the reinforcement scheme proposed in this paper, the mechanical behaviour of the surrounding strata and existing bridge piles caused by shield tunnelling after reinforcement were analyzed.

3.3.1. Surface Settlement

After the shield tunnelling is out of the scope of influence on the pile, the cloud diagram of surface settlement is as shown in Figure 8. The maximum surface settlement after excavation is 19.4 mm. Outside the 2D range from the tunnel centre (D is the tunnel

diameter), the surface deformation is not affected, and the influence range of the settlement trough is about 60 m. Although the diameter of the shield is substantial, the influence of excavation disturbance on the stratum is weakened because grouting enhances the characteristics of the soil.

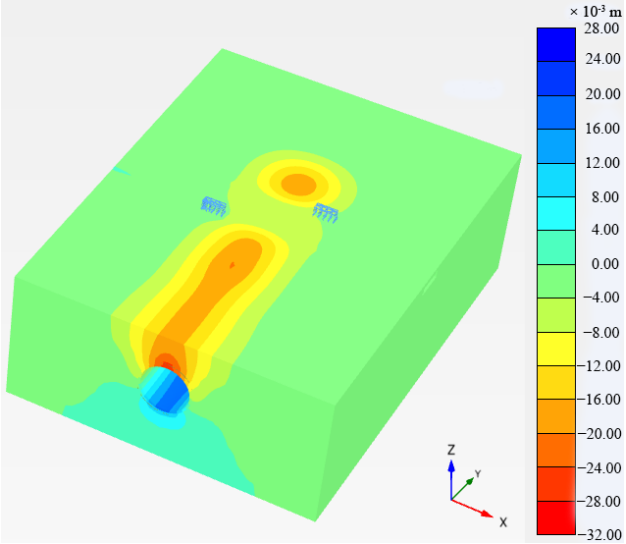

Figure 8. Map of the entire model settlement.

3.3.2. Displacement of Bridge Piles

Pile #2 and pile #3 nearest the shield tunnel (see Figure 7) were selected for analysis. Figure 9 shows the horizontal and vertical displacement and deformation of pile #2. It can be seen from the figure that the vertical displacement of pile #2 decreases with the deepening of the pile body, and the maximum vertical displacement is 2.1 mm at the pile top. This may lead to additional compressive stress in the vertical direction of the piles and reduce the bearing capacity of the piles. The horizontal deformation of the pile body is related to the relative position of the tunnel. The upper half of the pile body is deformed towards the tunnel side due to the volume loss during shield tunnelling, while the lower half of the pile body is deformed away from the tunnel side. The maximum horizontal displacement occurs at 5 m of the pile body, which is 0.5 mm. Similar to the deformation of pile #2, the vertical displacement of pile #3 decreases with the deepening of the pile body, and the maximum vertical displacement is 3.0 mm at the pile top. Within 18 m of the upper half of the pile, affected by the volume loss during shield tunnelling, it deforms towards the tunnel side, while the rest of the pile deforms away from the tunnel side. The maximum horizontal displacement occurs at 6 m of the pile body, which is 0.7 mm.

Figure 10 shows the internal force of pile #2 after excavation. It can be seen from the figure that the axial force of the pile is −500~−4681 kN, and the whole is in a compression state. Under the influence of negative friction within 7.5 m below the pile top, the pile body of the axial force tunnel increases with the deepening of the pile body, while within 7.5~23 m below the pile top, the pile body of the axial force tunnel decreases with the deepening of the pile body. Affected by the horizontal displacement of the pile body, the bending moment of the pile body in the direction perpendicular to the tunnel is more significant than that in the direction parallel to the tunnel. The maximum bending moment occurs at the 4 m position of the pile body, which is 83 kN·m. Figure 10 also shows the internal force of pile #3 after excavation. It can be seen from the figure that the axial force of the pile is −500~−4577 kN, and the whole pile is under compression. Under the influence of negative friction within 5m below the pile top, the pile body of the axial force tunnel increases with the deepening of the pile body, while within 5~23 m below the pile top, the pile body of the axial force tunnel decreases with the deepening of the pile body. The maximum bending moment of the pile body is 138 kN·m, which occurs at the position of

16m of the pile body. Generally speaking, the stress and displacement of pile #3 are similar to that of pile #2, but the stress and displacement are more significant than that of pile #2.

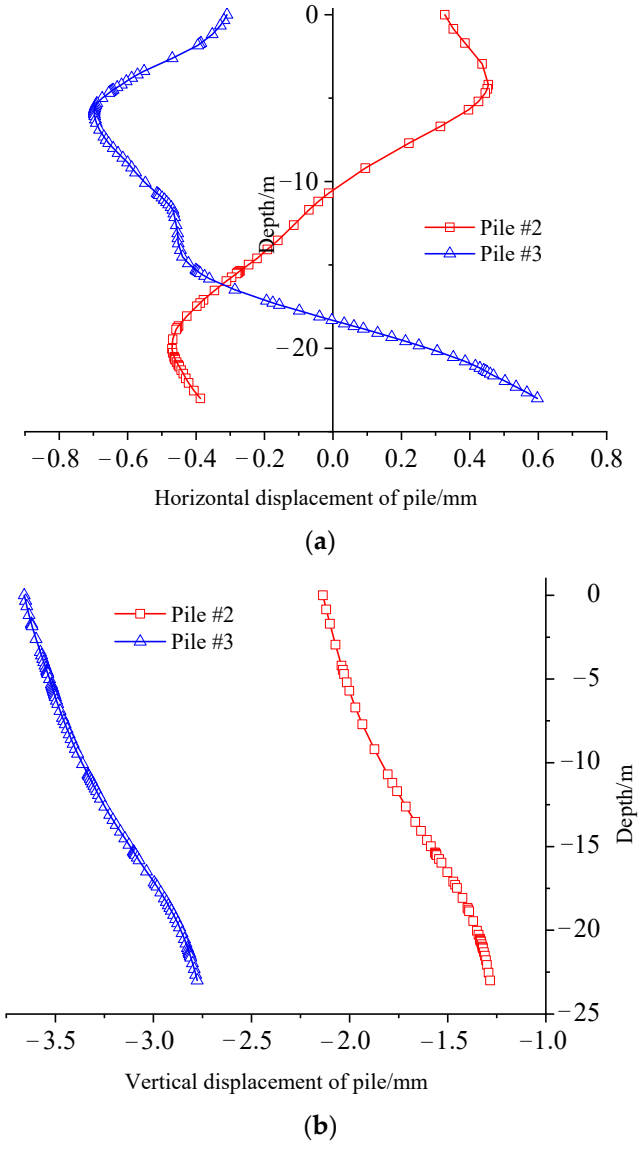

Figure 9. Deformation of piles #2 and #3. (**a**) Horizontal displacement. (**b**) Vertical displacement.

Due to the grouting reinforcement treatment of the soil around the pile body, the stiffness of the surrounding soil layer is improved so that the surface settlement and the horizontal and vertical displacement of the pile can meet the deformation control standard. In the process of side crossing bridge pile excavation of the shield tunnel, the shield tunnelling attitude is controlled, and the tunnel face pressure is controlled to achieve continuous, balanced and stable construction. At the same time, synchronous grouting and grouting behind the wall is strengthened to avoid significant disturbance to the stratum, and the assembly quality of segments is strictly guaranteed.

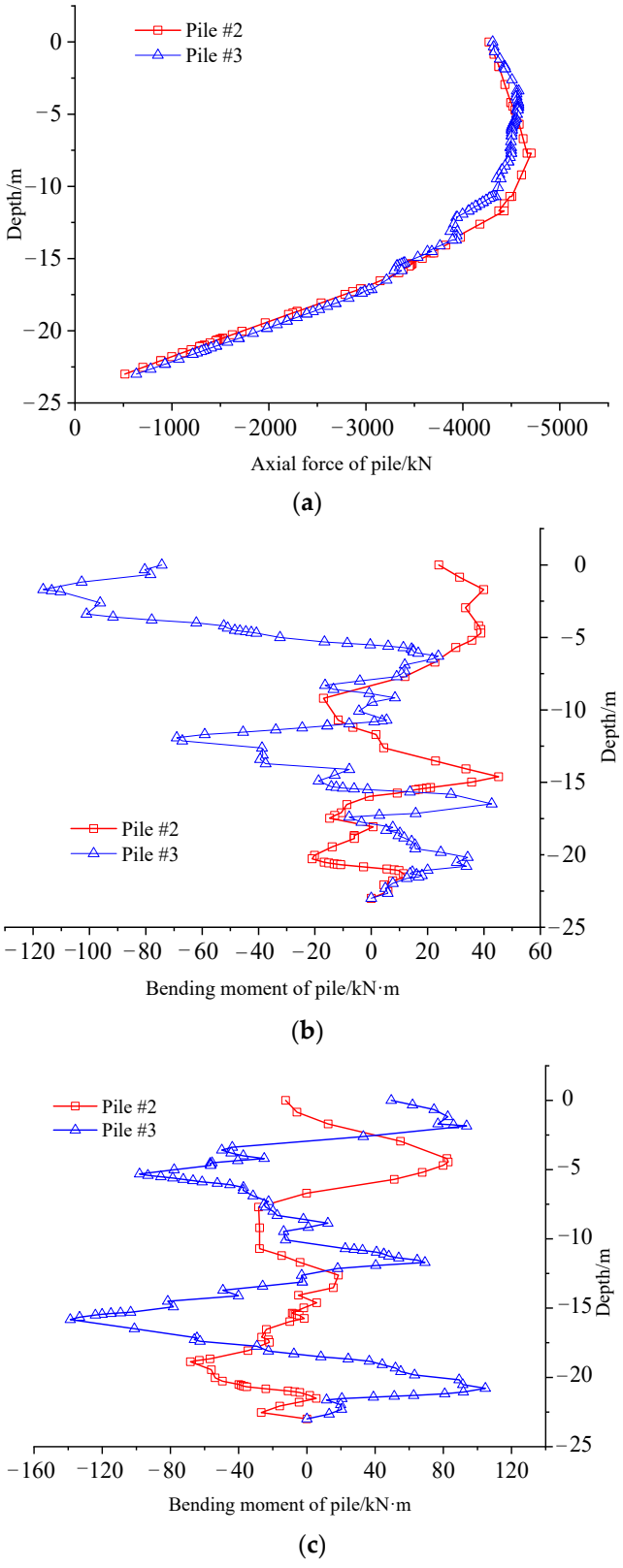

Figure 10. Internal forces in piles #2 and #3. (**a**) Axial force. (**b**) Bending moment parallel to tunnel direction. (**c**) Bending moment in vertical tunnel direction.

4. Field Measurement and Verification of Large Diameter Adjacent Shield Tunnelling Bridge Piles

4.1. Monitoring Scheme

Figure 11 shows the layout of bridge piles and surface monitoring points. One surface heave and subsidence monitoring point are set every 5 m along the longitudinal direction of the surface above the tunnel, and one group of surface monitoring sections is set every 10 m. Settlement and inclination monitoring points are set on the bridge piles. A group of segment lining deformation monitoring points is set every five rings in the shield tunnel. Local adjustments are made according to the surrounding environment in the actual construction process.

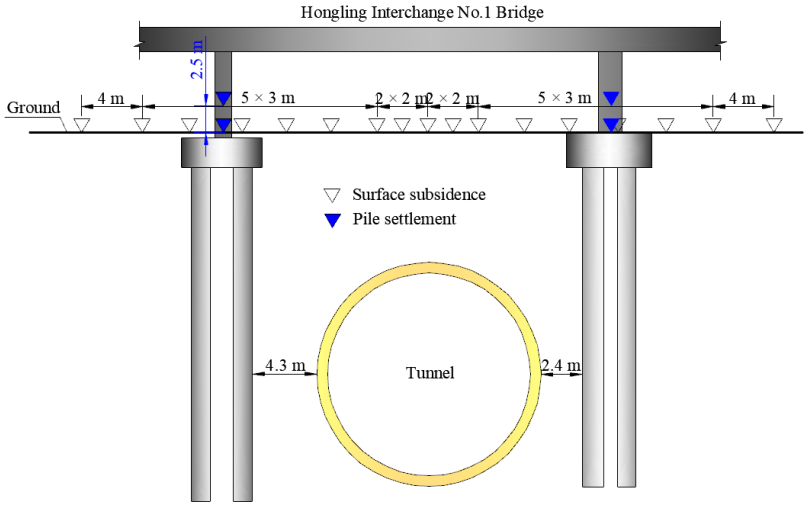

Figure 11. Layout of monitoring points.

4.2. Analysis of In-Site Monitoring Results

Figure 12 shows the vertical displacement of #2 and #3 bridge piles during the shield crossing of No. 1 bridge of Hongling Interchange. The monitoring value 30 m before shield crossing was taken as the initial value to analyze the impact on bridge piles during shield crossing. Before the shield passed through the bridge pile, the maximum vertical displacement of the bridge pile was −0.84 mm. Before the shield cutter head was driven from the bridge pile to the corresponding segment out of the shield tail, the slurry pressure and synchronous grouting pressure slightly higher than the theoretical value caused the bridge pile to float temporarily. After the shield tail passed through, the bridge pile sank about 1 mm. Through the secondary supplementary grouting measures, the bridge pile floated again. After the grouting was stopped, the monitoring value of the bridge pile had a cumulative settlement of 5 mm until the cutter head was 80 m away from the monitoring point. The maximum vertical displacement during excavation was −1.48 mm, which is less than the value of numerical simulation analysis to achieve a good reinforcement effect.

Figure 13 shows the surface settlements of different chainages at the position of the excavation surface during the period from 30 m in front of the No. 1 bridge of Hongling Interchange to 80 m after the shield crossing. Pile #3 of No. 1 bridge of Hongling Interchange is located at ZK0 + 890, and the corresponding chainage of pile #2 is ZK0 + 875. Within 30 m before the cutter head crossed, the surface settlement value of the upper part of the tunnel fluctuated slightly. With the continuous advancement of the shield machine, the ground surface was slightly uplifted. At this time, the pressure at the top of the slurry sump was 1.14~1.16 bar. When the shield cutter head was driven below the monitoring point, the ground surface sank slightly; the settlement value was 0.5 mm, and the corresponding pressure at the top of the slurry silo was 1.18 bar. When the segment below the monitoring point was out of the shield tail, a large settlement occurred at the surface monitoring points near the two bridge piles, and the average synchronous grouting amount in this process

was 100%. With the continuous tunnelling of the shield, the surface settlement gradually stabilised; the maximum settlement was ZK0 + 895, and the settlement was 35 mm. The ZK0 + 890–900 surface had a significant degree of settlement compared with the surface within the scope of bridge pile reinforcement, indicating that bridge pile reinforcement reduced the disturbance impact of shield construction on the soil. Compared with the numerical simulation value, the on-site monitoring value was smaller, mainly because the grouting measures could be controlled according to the real-time settlement during the construction process to control the pile deformation effectively.

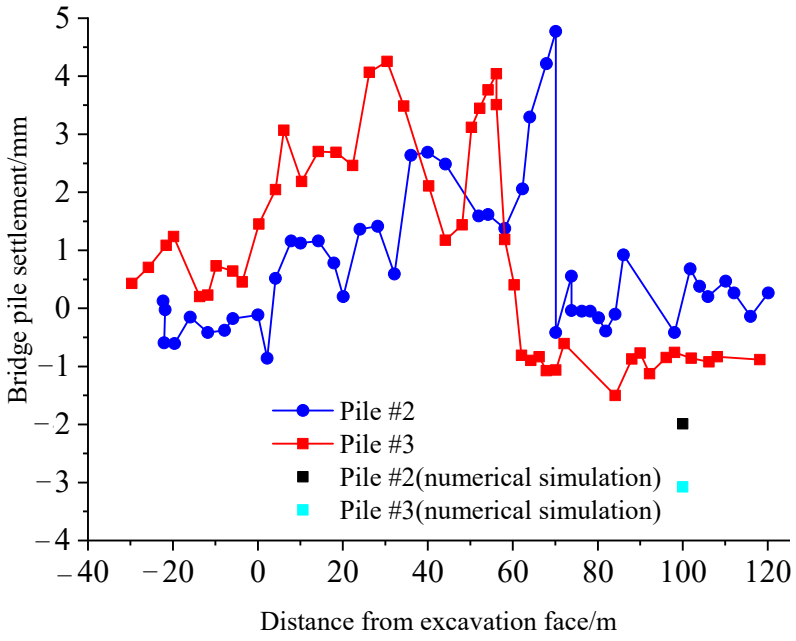

Figure 12. Vertical displacement of bridge piles.

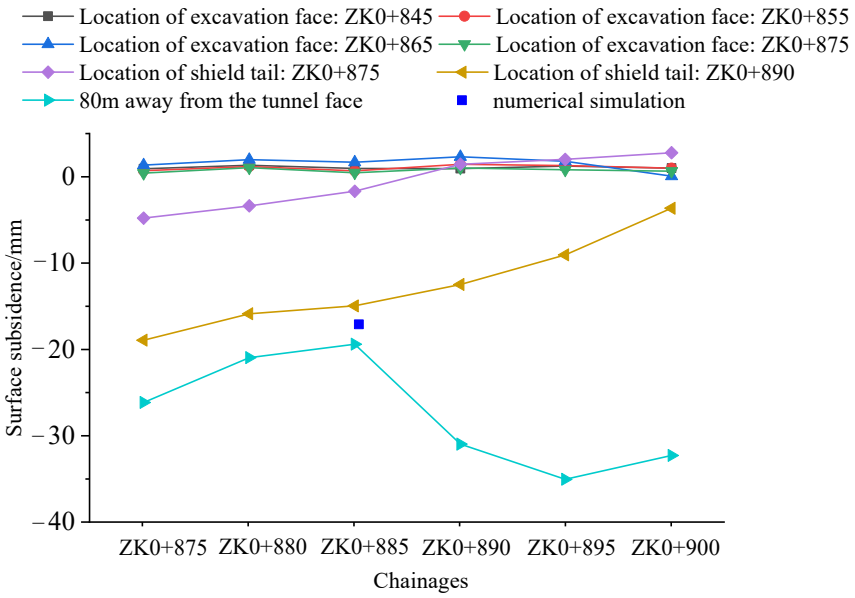

Figure 13. Surface settlements of different chainages.

Figure 14 shows the vertical displacement change of the tunnel vault after the shield passes. After the last section, the supporting trolley started to monitor the displacement of the arch crown after crossing through and stopped monitoring after the shield was

advanced by 350 m. The maximum displacement of the arch crown was −2.6 mm and finally stabilized at about −1.3 mm.

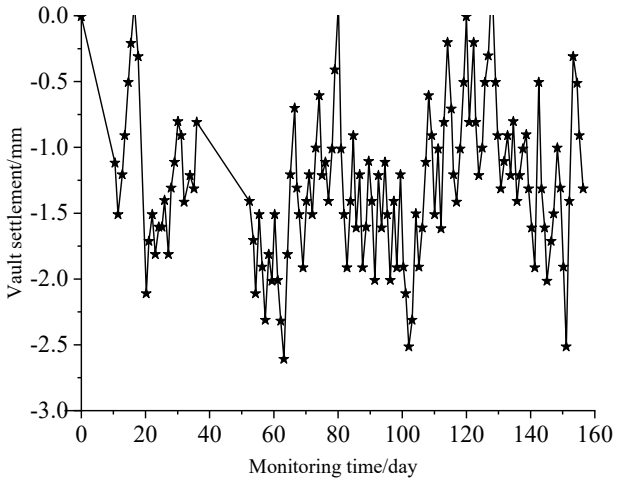

Figure 14. Vertical displacement of the tunnel vault.

4.3. Control of Tunnelling Parameters during Shield Machine Crossing Bridge Piles

The tunneling parameters must be controlled during the shield crossing the bridge pile. The tunnelling parameters, in this case, are shown in Table 5.

Table 5. The shield tunnelling parameters.

Top Pressure of Slurry Silo (Bar)	Total Thrust (kN)	Advance Rate (mm/min)	Cutter Head Speed (rad/min)	Cutter Head Torque (kN·m)
1.18~1.12	52,920~62,600	6~13	1.2	11,200~16,110

5. Conclusions

We used PLAXIS 3D finite element software to study the impact of super large-diameter shield tunnel excavation on existing bridge piles. Combined with the construction monitoring data, the following conclusions are drawn:

(1) Sleeve valve pipe pre-grouting reinforcement between shield tunnel and bridge pile foundation. After shield tunnelling to strengthen the stratum, the maximum simulated surface settlement was 19.4 mm, and the influence range of the settlement groove was about 60 m. According to the field data of shield tunnelling monitoring points, the surface settlement of the pre reinforced stratum around the bridge pile was about 25 mm, which is slightly larger than the simulation value but meets the requirements of surface settlement control. The maximum surface settlement was 35 mm at the position of the unreinforced stratum near the bridge pile, indicating that the stratum reinforcement significantly reduced the impact of shield construction on the soil.

(2) After the super large diameter shield tunnel passed through the reinforced stratum, the vertical displacement of the pile decreased with the deepening of the pile body. The maximum vertical displacement of the simulated bridge pile was 3.0 mm at the pile top and 0.7 mm at 5~6 m of the pile body, and the stress of the bridge pile met the strength requirements. During the construction, settlement monitoring points were set on the bridge pile. During shield crossing, the final settlement of the bridge pile was stable to 1.48 mm after a small settlement before crossing, and floated for a short time, which is less than the numerical simulation analysis value, indicating that the grouting reinforcement between the tunnel and the pile foundation had a noticeable control effect on the pile displacement and achieved a good reinforcement effect.

(3) Through the pre reinforcement of Shield Crossing front sleeve valve pipe, the surface and bridge pile displacement met the deformation control standard, and the risk of

short-distance crossing bridge pile was generally controllable. If it is necessary to set reasonable tunnelling parameters before crossing, to strictly control the tunnelling attitude of the shield, pay attention to control the tunnel face pressure, adjust the slurry pressure in a timely manner, reduce disturbance to the soil, and achieve continuous, balanced and stable advancement.

(4) The successful crossing of the Hongling Interchange No. 1 bridge provides a theoretical basis and engineering practice for the 16 m super-large diameter shield to cross an existing bridge pile foundation in a short distance in composite stratum with uneven, soft and hard features. This has significance reference value for similar projects.

Author Contributions: Conceptualization, J.W. and J.Z.; methodology, Z.T.; software, X.W.; validation, X.L., M.L. and Z.T.; formal analysis, J.Z.; investigation, J.W.; data curation, J.W.; writing—original draft preparation, J.Z.; writing—review and editing, J.W.; visualization, X.W.; supervision, M.L.; project administration, X.L. All authors have read and agreed to the published version of the manuscript.

Funding: This research received no external funding.

Institutional Review Board Statement: The participant's personal identification information used in the study did not include personal information. Ethical review and approval were not required for the study.

Informed Consent Statement: Not applicable.

Data Availability Statement: Data sharing is not applicable.

Acknowledgments: The authors would like to thank the anonymous reviewers for their valuable comments that helped improve the paper's quality. We also thank Beijing General Municipal Engineering Design & Research Insititute Co., Ltd. for helping us collect research data.

Conflicts of Interest: The authors declare no conflict of interest.

References

1. Jin, D.; Zhang, Z.; Yuan, D. Effect of dynamic cutterhead on face stability in EPB shield tunnelling. *Tunn. Undergr. Space Technol.* **2021**, *110*, 103827. [CrossRef]
2. Jin, D.; Yuan, D.; Li, X.; Su, W. Probabilistic analysis of the disc cutter failure during TBM tunnelling in hard rock. *Tunn. Undergr. Space Technol.* **2021**, *109*, 103744. [CrossRef]
3. Marshall, A.M. Tunnel-Pile Interaction Analysis Using Cavity Expansion Methods. *J. Geotech. Geoenviron. Eng.* **2012**, *138*, 1237–1246. [CrossRef]
4. Franza, A.; Losacco, N.; Ledesma, A.; Viggiani, G.M.B.; Jimenez, R. Protecting surface and buried structures from tunnelling using pile walls: A prediction model. *Can. Geotech. J.* **2020**, *58*, 1590–1602. [CrossRef]
5. Sirivachiraporn, A.; Phienwej, N. Ground movements in EPB shield tunnelling of Bangkok subway project and impacts on adjacent buildings. *Tunn. Undergr. Space Technol.* **2012**, *30*, 10–24. [CrossRef]
6. Jeon, Y.J.; Jeon, S.C.; Jeon, S.J.; Lee, C.J. Study on the behaviour of pre-existing single piles to adjacent shield tunnelling by considering the changes in the tunnel face pressures and the locations of the pile tips. *Geomech. Eng.* **2020**, *21*, 187–200.
7. Huang, K.; Sun, Y.-W.; Zhou, D.-Q.; Li, Y.-J.; Jiang, M.; Huang, X.-Q. Influence of water-rich tunnel by shield tunnelling on existing bridge pile foundation in layered soils. *J. Cent. South Univ.* **2021**, *28*, 2574–2588. [CrossRef]
8. Huang, F.; Wang, Z.; Zhang, M.; Li, S. Failure Mechanism of the Bearing Stratum at the End of a Pile Induced by Shield Tunnel Excavation Beneath a Piled Building. *KSCE J. Civ. Eng.* **2022**, *26*, 942–954. [CrossRef]
9. Berthoz, N.; Branque, D.; Wong, H.; Subrin, D. TBM soft ground interaction: Experimental study on a 1 g reduced-scale EPBS model. *Tunn. Undergr. Space Technol.* **2018**, *72*, 189–209. [CrossRef]
10. Song, G.; Marshall, A.M. Tunnel–piled structure interaction: Numerical simulation of hybrid centrifuge tests. *Comput. Geotech.* **2021**, *140*, 104477. [CrossRef]
11. Chaipanna, P.; Jongpradist, P. 3D response analysis of a shield tunnel segmental lining during construction and a parametric study using the ground-spring model. *Tunn. Undergr. Space Technol.* **2019**, *90*, 369–382. [CrossRef]
12. Wang, Z.; Zhang, K.-W.; Wei, G.; Li, B.; Li, Q.; Yao, W.-J. Field measurement analysis of the influence of double shield tunnel construction on reinforced bridge. *Tunn. Undergr. Space Technol.* **2018**, *81*, 252–264. [CrossRef]
13. Nematollahi, M.; Dias, D. Three-dimensional numerical simulation of pile-twin tunnels interaction—Case of the Shiraz subway line. *Tunn. Undergr. Space Technol.* **2019**, *86*, 75–88. [CrossRef]
14. He, S.; Lai, J.; Li, Y.; Wang, K.; Wang, L.; Zhang, W. Pile group response induced by adjacent shield tunnelling in clay: Scale model test and numerical simulation. *Tunn. Undergr. Space Technol.* **2022**, *120*, 104039. [CrossRef]

15. Wang, J.; Wen, Z. Analysis of Construction Impact of a Large Diameter Shield Tunnelling Side-Crossing Viaduct Pile Foundations in Short Distance. *Geotech. Geol. Eng.* **2021**, *39*, 5587–5598. [CrossRef]
16. Professional Standards Compilation Group of People's Republic of China. *Code for Design of Road Tunnel (JTG D70-2004)*; China Communications Press: Beijing, China, 2004.
17. Xiong, Q.; Mo, Y. Discussion on the Key Technologies for Survey of Super Large Diameter Urban Shield Tunnel Under Complex Conditions—Taking Chunfeng Tunnel as an Example. *Constr. Des. Proj.* **2019**, *16*, 90–91. (In Chinese)
18. Zhang, W. Research on Deformation and Control of Bridge Pile Structure of Large Diameter Shield Tunnel under Airport Line of Beijing Metro Line 14. Master's Thesis, Beijing Jiaotong University, Beijing, China, 2012.
19. Lueprasert, P.; Jongpradist, P.; Jongpradist, P.; Suwansawat, S. Numerical investigation of tunnel deformation due to adjacent loaded pile and pile-soil-tunnel interaction. *Tunn. Undergr. Space Technol.* **2017**, *70*, 166–181. [CrossRef]
20. Vu, M.N.; Broere, W.; Bosch, J. Effects of cover depth on ground movements induced by shallow tunnelling. *Tunn. Undergr. Space Technol.* **2015**, *50*, 499–506. [CrossRef]
21. Sheng, M.; Gao, J.; Guo, P.; Cao, R.; Wang, Y. Temporal-Spatial Characteristics of Ground and Pile Responses to Twin Shield Tunnelling in Clays. *Geofluids* **2021**, *2021*, 2373456. [CrossRef]
22. Xu, Q.; Zhu, H.; Ma, X.; Ma, Z.; Li, X.; Tang, Z.; Zhuo, K. A case history of shield tun-nel crossing through group pile foundation of a road bridge with pile underpinning technologies in Shanghai. *Tunn. Undergr. Space Technol.* **2015**, *45*, 20–33. [CrossRef]
23. Mohamad, W.; Bourgeois, E.; Le Kouby, A.; Szymkiewicz, F.; Michalski, A.; Branque, D.; Berthoz, N.; Soyez, L.; Kreziak, C. Full scale study of pile response to EPBS tunnel-ling on a Grand Paris Express site. *Tunn. Undergr. Space Technol.* **2022**, *124*, 104492. [CrossRef]
24. Liu, C.; Zhang, Z.; Regueiro, R.A. Pile and pile group response to tunnelling using a large diameter slurry shield—Case study in Shanghai. *Comput. Geotech.* **2014**, *59*, 21–43. [CrossRef]
25. Liu, B.; Yu, Z.; Yao, B.; Han, Y.; Liu, H.; Wang, S. Responses of the ground and adja-cent pile to excavation of U-shaped tunnel. *Comput. Geotech.* **2021**, *130*, 103919. [CrossRef]
26. Andreotti, G.; Calvi, G.M.; Soga, K.; Gong, C.; Ding, W. Cyclic model with damage assessment of longitudinal joints in segmental tunnel linings. *Tunn. Undergr. Space Technol.* **2020**, *103*, 103472. [CrossRef]
27. Tvede-Jensen, B.; Faurschou, M.; Kasper, T. A modelling approach for joint rotations of segmental concrete tunnel linings. *Tunn. Undergr. Space Technol.* **2017**, *67*, 61–67. [CrossRef]
28. Schanz, T. Formulation and verification of the Hardening-Soil Model. *RBJ Brinkgreve Beyond 2000 Comput. Geotech.* **1999**, 281–290.
29. Benz, T. Small-Strain Stiffness of Soils and Its Numerical Consequences. Ph.D. Thesis, University of Stuttgart, Baden-Württemberg, Germany, 2007.
30. Honkanadavar, N.P.; Sharma, K.G. Modeling the triaxial behavior of riverbed and blasted quarried rockfill materials using hardening soil model. *J. Rock Mech. Geotech. Eng.* **2016**, *8*, 350–365. [CrossRef]
31. Sukkarak, R.; Likitlersuang, S.; Jongpradist, P.; Jamsawang, P. Strength and stiffness parameters for hardening soil model of rockfill materials. *Soils Found.* **2021**, *61*, 1597–1614. [CrossRef]
32. Seyedan, S.; Sołowski, W.T. Enhancing Constitutive Models for Soils: Adding the Capability to Model Nonlinear Small Strain in Shear. *Adv. Civ. Eng.* **2019**, *2019*, 6016350. [CrossRef]
33. Beijing General Municipal Engineering Design & Research Insititute Co., Ltd. *Geological Exploration Report of Chunfeng Tunnel*; Beijing General Municipal Engineering Design & Research Insititute Co., Ltd.: Beijing, China, 2018.
34. Brinkgreve, R.B.J.; Broere, W. *Plaxis Material Models Manual*; PLAXIS B V: Delft, The Netherlands, 2006.
35. Zhou, Z.; Zhao, J.; Tan, Z.; Zhou, X. Mechanical responses in the construction process of super-large cross-section tunnel: A case study of Gongbei tunnel. *Tunn. Undergr. Space Technol.* **2021**, *115*, 104044. [CrossRef]
36. Russo, G. Evaluating the Required Face-Support Pressure in Epbs Advance Mode. *Gallerie E Grandi Opere Sotter.* **2003**, *71*, 1–14.
37. Oh, J.Y.; Park, H.; Kim, D.; Chang, S.; Lee, S.; Choi, H. Study on the effect of tail void grouting on the short-and long-term surface settlement in the shield TBM Tunnelling using numerical analysis. *J. Korean Tunn. Undergr. Space Assoc.* **2017**, *19*, 265–281. [CrossRef]